

Corrosion Inhibitors for Carbon Steel in HCl Environment: Synthesis and Characterization of Trimethoprim-Metal Complexes

Ali Abra NASER¹, Hassan HAMMED², Ammar Zeidan ALSHEMERY^{3*, 4, 5, 6, 7}, İsmail Seçkin ÇARDAKLI⁸

¹ Ministry of Education-General Directorate of Misan Education, Misan 62001, Iraq

² Ministry of Interior Affairs-General Directorate of Misan Police, Misan 62001, Iraq

³ Nanomaterials Research Center, Department of Chemistry, College of Science, Mathematics and Technology, Wenzhou-Kean University, 88 Daxue Road, Ouhai, Wenzhou 325060, Zhejiang Province, China.

⁴ Wenzhou Municipal Key Lab for Applied Biomedical and Biopharmaceutical Informatics, Ouhai, Wenzhou 325060, Zhejiang Province, China

⁵ Zhejiang Bioinformatics International Science and Technology Cooperation Center, Ouhai, Wenzhou 325060, Zhejiang Province, China

⁶ Dorothy and George Hennings College of Science, Mathematics and Technology, Kean University, 1000 Morris Ave, Union, NJ 07083, USA

⁷ Biomedical Engineering Department, College of Engineering and Technologies, Al-Mustaqbal University, Hillah 51001, Babil, Iraq

⁸ Department of Metallurgical and Materials Engineering, Atatürk University, Erzurum, 25240, Turkey

<http://doi.org/10.5755/j02.ms.36133>

Received 22 January 2024; accepted 7 March 2024

This study is about making and figuring out what trimethoprim (TM), a popular corrosion inhibitor, is like and then using it as an inhibiting agent to stop corrosion in carbon steel in acid media (HCl solution) through adsorption. TM has also been known as the prevalent anti-corrosive agent. It can be added to a liquid or gas to slow the pace of a chemical reaction (in the case of a material – typically a metal or alloy – that corrodes when it encounters the fluid). Many antibiotic compounds, such as TM derivatives, diiron salt dihydrate, and diiron salt tetrahydrate, have active groups that can stop metal from corroding. Spectroscopic methods like XRD (X-ray diffraction), FTIR (Fourier transform infrared spectroscopy), UV-visible (ultraviolet-visible spectroscopy), and TGA (thermogravimetric analysis) were used to study the TM drug. Similarly, the OCP (open circuit voltage) technique was introduced to assess the corrosion resistance and the density of current vs. voltage. Finally, this study revealed that TM drugs could be suggested for introduction as corrosion inhibitors due to their simple production and the fact that they have many active groups that exhibit the ability to coordinate with carbon steel. Our study revealed that changes in inhibitor concentrations, the solution's acidity, and the metal's surface area all contribute to adsorption.

Keywords: corrosion, trimethoprim, carbon steel.

1. INTRODUCTION

Corrosion is a natural process when the metal reacts with its surrounding environment, deteriorating its properties. Uniform corrosion is a prevalent type of deterioration observed in carbon steel, which occurs when the metal corrodes uniformly over its surface. This type of corrosion is often caused by exposure to acidic [1]. Another type of corrosion in carbon steel is pitting corrosion, which involves the localized breakdown of the metal surface in small pits or holes. Pitting corrosion is often caused by exposure to chloride ions or other aggressive environments [2]. Various measures can be taken to prevent corrosion in carbon steel, including corrosion inhibitors, protective coatings, and cathodic protection. It's also essential to select the appropriate material for the specific environment and application and to properly maintain and inspect the equipment to identify and address any corrosion issues as soon as possible.

There are two primary types of corrosion inhibitors for carbon steel: inorganic and organic. Metal ions or metal salts, which are inorganic inhibitors, often create a protective coating on the metal's surface to prevent corrosion. Some common examples of inorganic inhibitors for carbon steel include chromates, phosphates, and silicates [3–5]. These inhibitors are effective in alkaline environments but may be less effective in acidic environments [6]. Conversely, organic inhibitors are usually organic molecules that adhere to the metal surface, forming a protective barrier that inhibits corrosion. Some common examples of organic inhibitors for carbon steel include amines, imidazoles, and organic acids [7, 8]. These inhibitors are effective in acidic and neutral environments but may be less effective in alkaline environments [6].

The capability of various drugs to serve as inhibitors for carbon steel corrosion has been explored. These medications, which are often organic substances, can stick

* Corresponding author. Tel.: +860-577-55870390; fax: +860-577-55870390. E-mail: aalshema@kean.edu (A.Z. Alshemary)

to metal surfaces and form a barrier that prevents corrosion. Ibuprofen, for example, has demonstrated efficacy in halting the deterioration of carbon steel in acidic environments [9]. Paracetamol (acetaminophen) is believed to prevent carbon steel corrosion in acidic environments by forming a protective layer on the metal surface through its interaction with metal ions [10]. This action is thought to occur as the drug adheres to the surface, establishing a barrier that prevents additional corrosion.

Trimethoprim, a synthetic antibiotic drug, has been studied for its potential as a corrosion inhibitor for carbon steel in acidic conditions. It is believed that trimethoprim's chemical structure, which contains nitrogen atoms and aromatic rings, allows it to bind to the metal surface, creating a protective coating that prevents corrosion [11]. Research indicates trimethoprim can prevent carbon steel corrosion in acidic settings [12]. The efficiency of trimethoprim as a corrosion inhibitor is influenced by variables like the concentration of trimethoprim and the environmental temperature [12]. The mechanism by which trimethoprim inhibits corrosion has yet to be fully understood. The mechanism behind trimethoprim's ability to inhibit corrosion is thought to entail adsorption onto the metal surface and forming a protective layer. The involvement of nitrogen atoms and aromatic rings in the trimethoprim molecule may facilitate the formation of a coordination complex with metal ions present in the solution, thereby amplifying its corrosion-inhibitory effects [11].

Although trimethoprim exhibits potential as a corrosion inhibitor for carbon steel, additional studies are necessary to assess its effectiveness comprehensively and to refine its application in real-world scenarios. In this work, trimethoprim derivative-metal complexes were prepared and characterized using different techniques, then evaluated its ability as a preventive agent against the corrosion of carbon steel alloy in acidic conditions.

2. EXPERIMENTAL DETAILS

2.1. Materials

N,N'-(5-(3,4,5-trimethoxybenzyl)pyrimidine-2,4 dial) bis (3,4,5-trihydroxy benzamide), and N,N'-(5-(3,4,5-trimethoxybenzyl)pyrimidine-2,4-dial) bis (azanediyl) bis (carbonothioyl) bis (3,4,5 trihydroxy benzamide) were prepared and characterized in our previous study [13] – carbon steel alloy C1025. Ethanol, methanol, and iron (III) chloride were used as received without further purification.

2.2. Preparation of compounds

In this study, two compounds were successfully prepared. Briefly, Comp-1 was prepared by dissolving 0.562 g of N, N'-(5-(3,4,5-trimethoxybenzyl) pyrimidine-2,4-dial) bis (3,4,5-trihydroxy benzamide) in 20 mL of ethanol, then mixing with FeCl₂·3H₂O solution (0.556 g dissolved in 10 mL of double distilled water (DDW) for 3 hr at 55 °C. The black precipitation was collected through filtration, washed several times using DDW, and dried in the oven. The yield was about 72 %, and mp was found at over 300 °C. The second compound (Comp-2) was prepared by dissolving 0.712 g of N, N'-(5-(3,4,5-

trimethoxybenzyl)pyrimidine-2,4diyl) bis (azanediyl) bis (carbonothioyl) bis (3,4,5–trihydroxy benzamide) in 20 mL of methanol and heating for a few minutes. Then I added this to the FeCl₂·3H₂O solution (0.556 g dissolved in 10 mL of DDW). This mixture was stirred for 3 hr while heating at 50 °C. The final black solid product was filtered, repeatedly washed with DDW, and then oven-dried. Subsequently, the yield was calculated to be approximately 80 %, and the melting point (MP) was determined to be between 244 and 242 °C.

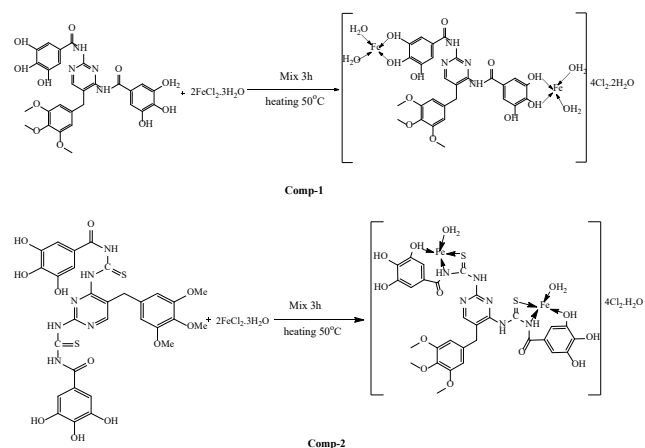


Fig. 1. Preparation of compounds

2.3. Preparation of working electrodes

Carbon steel rods (C1025) were utilized with the following dimensions: 2.55 cm wide, 2 cm long, and 0.35 cm thick. Their total surface area was around 12.4925 cm². These rods were immersed in the solution and then ground with increasing grades of silicon carbide. The alloy was then dried, cleaned with DDW, acetone, and ethanol, and then packed in silica gel-filled desiccants for storage in a dry location at room temperature.

2.4. Tafel plot and electrochemical cells

An open circuit voltage (OCP) technique was introduced for 20 minutes to test the corrosion resistance and the density of current vs. voltage. A potentiated/galvanostatic control computer was used to scan the potential range between - 2.5 and + 2.5 mV (against OCP) at a rate of 10 mV s⁻¹ to produce the polarization curve. During this study, we used an electrochemical cell that has a 100 mL vessel connected to three electrodes in this order: a carbon steel electrode, a platinum electrode, and a saturated calomel electrode.

2.5. Instrumentation

The prepared complexes were identified and characterized using different techniques. The optical characteristics of the synthesized materials were assessed with an ultraviolet–visible spectrometer (model UV-9200, Biotech Engineering Management Co. LTD., UK). Thermal properties were examined through Thermogravimetric Analysis (model TGA Q500 V6.7, TA Instruments, USA). Fourier Transform Infrared Spectrometer (model FTIR-8400S, Shimadzu, Japan) was used to identify the functional groups. The elemental ratio of Carbon, Hydrogen, Nitrogen,

and Sulphur (CHNS) was determined using a CHNS Elemental Analyzer (model EA 3000, Euro vector, Italy).

3. RESULTS AND DISCUSSION

The UV/visible spectra of the complexes display two distinct regions (Fig. 2). The first region has a range (200–400 nm), which has been ascribed to correspond to $n \rightarrow \pi^*$ transition, and the second region has exhibited its capacity (400–800 nm) and was attributed to the presence of iron in the complex [14, 15]. According to the spectra displayed in Fig. 2, it can be inferred that both developed bands are characteristic of ligand field and charge transitions.

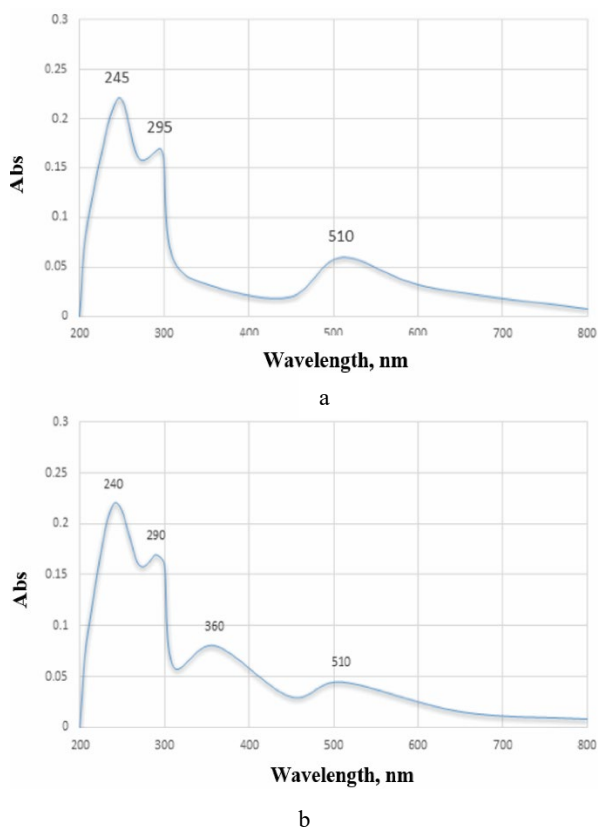


Fig. 2. UV/visible spectra: a–Comp-1 samples; b–Comp-2 samples

The TGA analysis was utilized to assess the stability and probe into the structural intricacies of the complex. Performed under a nitrogen atmosphere with a flow rate of 20 mL/min, the thermal examination spanned temperatures from 80 to 600 °C, with a consistent heating rate of 10 °C per minute. A two-phase weight loss pattern was seen by looking at the TGA curve of complex Comp-1 (shown in Fig. 3 a). The initial phase, occurring between 80–200 °C, exhibited a practical weight loss of 13.98 % (theoretical: 13.88 %), ascribed to the expletion of two crystalline and four coordinated water molecules [16]. The subsequent phase, ranging from 200–400 °C, demonstrated a 24.92 % weight loss in practice (theoretical: 23.27 %), corresponding to the loss of $C_{10}H_{13}O_3$.

On the other hand, the TGA curves for Comp-2 (shown in Fig. 3 b) showed a triphasic weight loss over a temperature range of 80–850 °C, which added up to a total

weight loss of about 93.32 %. The initial decrement, recorded between 80–150 °C, was 6.77 % in practice (theoretical: 6.27 %), attributable to the loss of a singular crystalline water molecule and two coordinated water molecules. The second decrement phase, spanning 150–390 °C, witnessed a practical weight loss of 30.25 % (theoretical: 29.88 %), presumably due to the elimination of $C_{13}H_{13}N_4O_2$. The final decrement phase, ranging from 390–850 °C, incurred a practical weight loss of 51.32 % (theoretical %), correlating with the loss of $C_{20}H_{16}N_4O_5S$. In addition to these weight losses, an ancillary decrement was observed, potentially linked to the thermally induced release of water molecules.

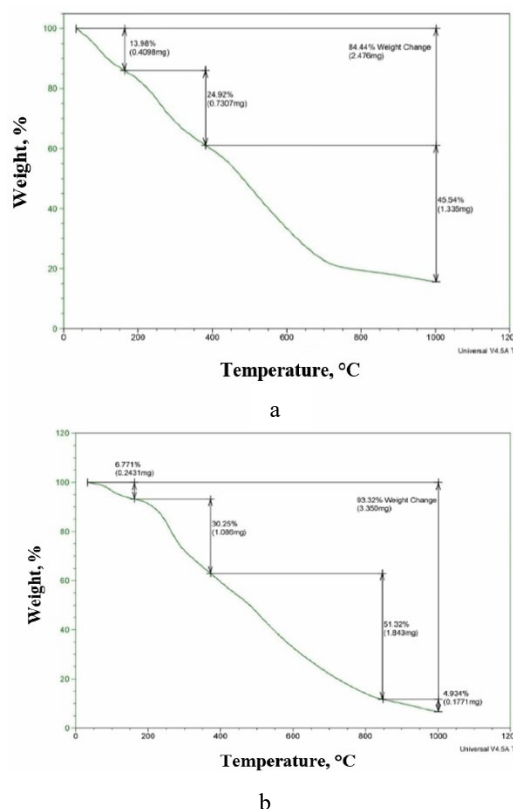
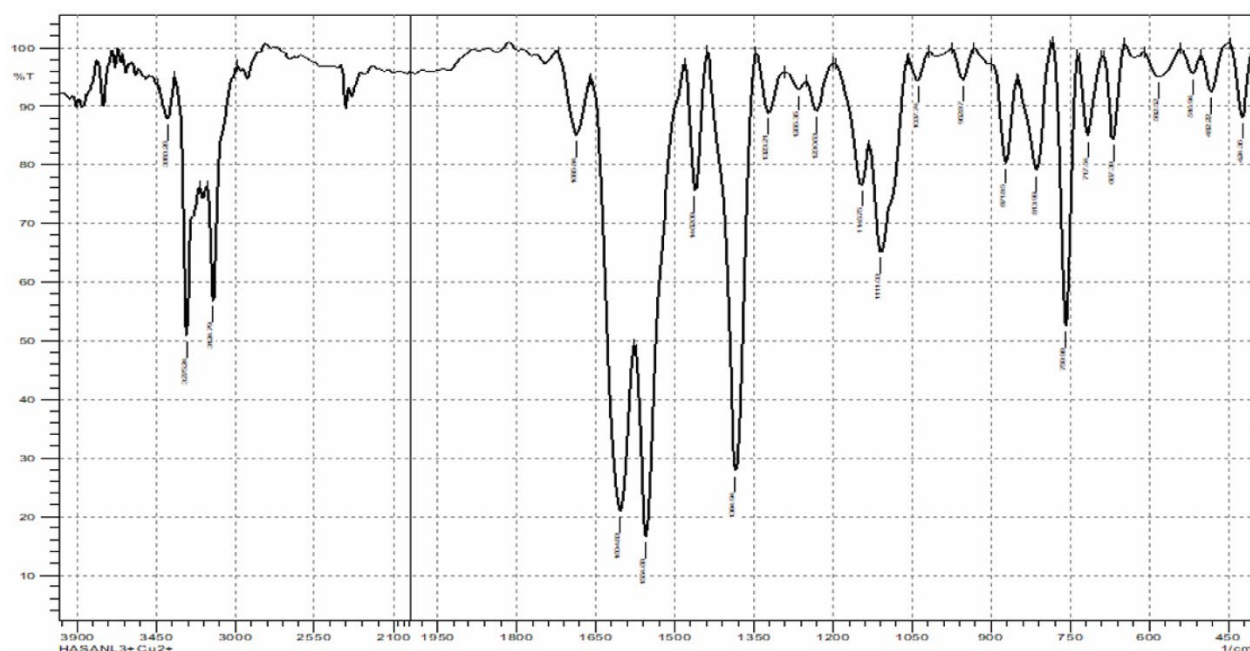


Fig. 3. TGA graph: a–Comp-1 samples; b–Comp-2 samples

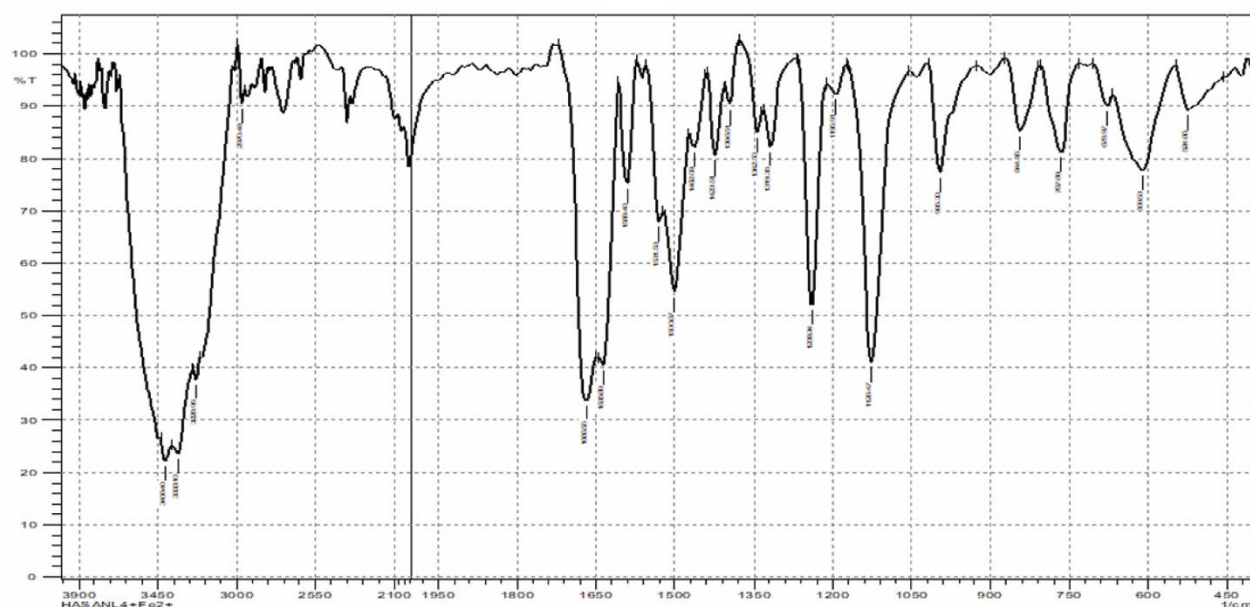
IR spectroscopy is an essential tool for studying the complexes that have been synthesized because it lets us find the places where the ligand and metal ion interact. IR spectral results can also be used to determine if the complex has functional groups and its crystallinity level. Table 1 compares the IR spectra of pure TM and metal complexes made during this research. The different IR deflection values result from how well the metal and ligand are bonded. The IR spectra of the complexes (Comp-1 and Comp-2) showed two broad bands at 3270 cm^{-1} and 3410 cm^{-1} , which were thought to be caused by the OH group stretching. At the same time, the bands within the 3120 to 3327 cm^{-1} ranges were recognized as the characteristic stretching vibration of the NH_2 group. While frequencies found around 1666 cm^{-1} and 1660 cm^{-1} , respectively, were attributed to the existence of influential groups C=O, The frequency band showing its manifestation around the frequency of 2080 cm^{-1} in the complex was considered due to group C=S (Fig. 4) [17–20].

Table 1. Spectral IR data of ligands and their complexes

	$\nu(\text{O-H}), \text{cm}^{-1}$	$\nu(\text{N-H}), \text{cm}^{-1}$	$\nu(\text{C=O}), \text{cm}^{-1}$	$\nu(\text{C=S}), \text{cm}^{-1}$	$\nu(\text{N-H bond}), \text{cm}^{-1}$	$\nu(\text{C-H Arom.}), \text{cm}^{-1}$	$\nu(\text{C-H al ph.}), \text{cm}^{-1}$	$\nu(\text{C-O}), \text{cm}^{-1}$	$\nu(\text{C-N}), \text{cm}^{-1}$	$\nu(\text{C-H bend.}), \text{cm}^{-1}$
TM	3367 (BR)	3290 (BR)	1701 (s)	–	1620 (m)	3070 (w)	2847 (w)	1450 (m) 1342 (m)	1246 (s)	1030 (m)
Comp-1	3270 (s)	3120 (br)	1666 (s)	–	1590 (m)	3010 (w)	2280 (w)	1442(m) 1390 (s)	1240 (s)	1111 (m)
Comp-2	3410 (br)	3327 (br)	1660 (s)	2080 (m)	1610 (m)	3042 (w)	2958 (w)	1420 (w) 1340 (w)	1260 (s)	1118 (m)



a



b

Fig. 4. IR spectra: a – Comp-1 samples; b – Comp-2 samples

The physical properties of two complexes, Comp-1 and Comp-2 are shown in Table 2. These properties include color, melting point (mp), conductivity ($\text{ohms}^{-1} \text{cm}^2 \text{mol}^{-1}$), and yield percentage. Firstly, both Comp-1 and Comp-2

exhibit a black coloration, which could indicate their molecular structure or the presence of certain elements or ligands within the complexes. Regarding the melting points, Comp-1 has a melting point of over 300°C , demonstrating

its high thermal stability. Such a characteristic can be advantageous in applications requiring the complex to maintain its structural integrity under elevated temperatures. On the other hand, Comp-2 has a melting point range of 244–242 °C. The slight range in the melting point could be attributed to impurities in the sample or experimental uncertainties. Still, overall, it indicates a good level of thermal stability, though less than that of Comp-1.

Table 2. Physical properties of the prepared complexes

	Color	M.p., °C	Ohm ⁻¹ Cm ² .mol ⁻¹	Yield, %
Comp-1	Black	Over 300	173.9	72
Comp-2	Black	244–242	185.7	80

The conductivity values provided for the two complexes are 173.9 ohm⁻¹ cm² mol⁻¹ for Comp-1 and 185.7 ohm⁻¹ cm² mol⁻¹ for Comp-2. These values suggest that both complexes have considerable ionic conductivity, with Comp-2 displaying slightly higher conductivity than Comp-1. There may be differences in how well they conduct electricity because of differences in their molecular structure or the types of ligands that are present, which can affect how easily charge carriers can move around in the complexes.

Lastly, the yield percentages are 72 % for Comp-1 and 80 % for Comp-2. These values indicate a relatively high efficiency in the synthesis of both complexes, with Comp-2 showing a slightly better yield. A higher yield is generally preferable as it implies a more efficient use of reactants, potentially leading to cost-effectiveness and less waste in a synthetic process.

Table 3 presents the results of the CHNS analysis for the two synthesized complexes, Comp-1 and Comp-2. It details the observed and calculated percentages of carbon (C), hydrogen (H), nitrogen (N), and sulfur (S). For Comp-1, with the empirical formula C₂₈H₃₄Fe₂N₄O₁₅, the found elemental percentages are as follows: 43.21 % C, 4.40 % H, 7.20 % N, and no sulfur content. In comparison, the calculated percentages are slightly higher for each

element: 43.37 % C, 4.47 % H, 7.27 % N. The discrepancies between the found and calculated values are minimal, suggesting a high degree of accuracy and reliability in the synthesis and characterization of Comp-1. However, the slight underestimation in the found values compared to the calculated values could be due to experimental errors, impurities, or incomplete purification.

Moving on to Comp-2, represented by the formula C₃₀H₃₂Fe₂N₆O₁₃S₂, the found elemental percentages are 41.88 % C, 3.75 % H, 9.77 % N, and 7.45 % S. The calculated percentages for this compound are 41.51 % C, 3.70 % H, 9.33 % N, and 7.83 % S. Here, observes a mixed trend. The found values for carbon and nitrogen are slightly higher than the calculated values, whereas the found values for hydrogen and sulfur are slightly lower. These discrepancies, though modest, could be indicative of experimental inaccuracies, impurities, or issues with sample preparation. The sulfur content is crucial to note as it is unique to Comp-2 and could play a significant role in its chemical properties and potential applications.

Various parameters, including the corrosion potential (E_{corr}), the cathodic and anodic potentials (c and a), and the corrosion current density (I_{corr}), were examined. The results showed a slight shift in the OCP values toward the negative side, which shows that inhibitors for TM derivatives are present. This behavior was attributed to the inhibitor's adsorption on the C1025 alloy or to the deposition of corrosion reaction products. The electrochemical data from Tafel plots in Table 4 and Fig. 5 a and b for carbon steel alloy (C1025) in 0.1 M HCl are shown.

The data comes from different concentrations of the synthetic inhibitors (Comp-1 and Comp-2). The Tafel plot data revealed significant changes in electrochemical parameters with increasing concentrations of the synthesized inhibitors. The corrosion current density (I_{corr}) significantly decreased when inhibitors were present, compared to their absence. This reduction is attributed to forming an adsorbed layer of inhibitors on the alloy's surface [21, 22].

Table 3. CHNS results for the prepared complexes

Sample ID	Formula	Elemental, %			
		C	H	N	S
Comp-1	C ₂₈ H ₃₄ Fe ₂ N ₄ O ₁₅	43.21 (43.47)	4.40 (4.47)	7.20 (7.27)	–
Comp-2	C ₃₀ H ₃₂ Fe ₂ N ₆ O ₁₃ S ₂	41.88 (41.51)	3.75 (3.70)	9.77 (9.33)	7.45 (7.83)

Table 4. Displays corrosion data with and without the inhibitors Comp-1 and Comp-2 at a temperature of 298 K

Comp	Conc, ppm	E _{corr} , mV	I _{corr} , μA.Cm ²	CR, mpy	β _a , mV	β _c , mV	R _p , Ω.cm ²	% IE	θ
HCl	Blank	-707	1011	468.37	228.93	-226.88	17.797	–	–
Comp-1	5	-615	606	280.62	269.43	-473.49	29.407	40	0.40
	10	-612	481	222.69	197.85	-280.05	37.431	52.4	0.53
	15	-612	405	187.39	283.91	-315.83	44.482	60.0	0.60
	20	-620	309	143.05	222.89	-482.13	58.269	69.5	0.69
	25	-614	299	138.44	138.44	156.55	-305.66	60.207	70.4*
Comp-2	5	-596	620	287.00	130.38	-153.56	29.044	38.7	0.38
	10	-609	472	218.58	222.95	-385.23	38.143	53.3	0.53
	15	-621	301	139.36	429.44	-884.85	59.813	70.2	0.70
	20	-602	208	96.316	163.25	-325.21	86.542	79.4	0.79
	25	-602	185	85.594	231.53	-489.06	97.383	81.7*	0.81

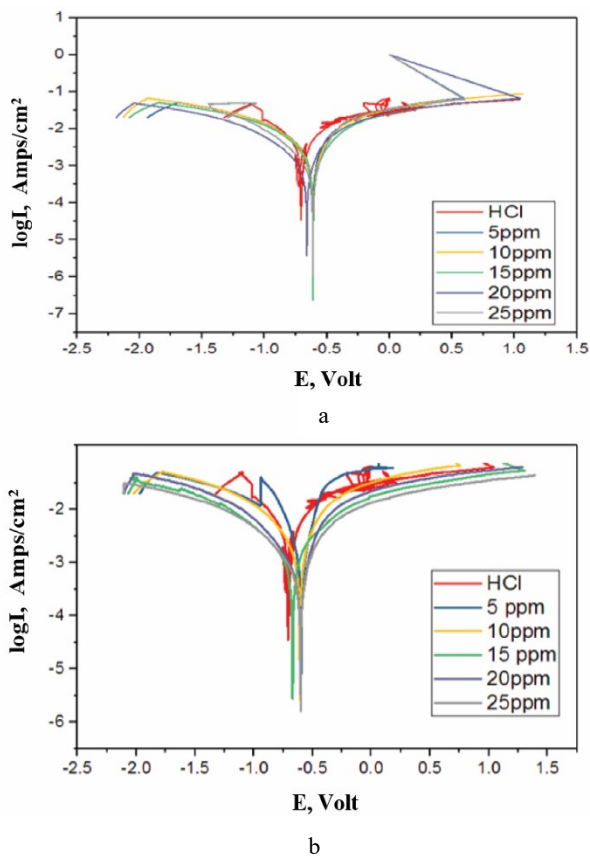


Fig. 5. Tafel plot of alloy in the presence and absence: a– Comp-1 at 298 K; b– Comp-2 at 298K

Meanwhile, the polarization resistance (R_p) of both Comp-1 and Comp-2 compounds increases with increasing inhibitor concentration [23]. The results also revealed that the corrosion potential (E_{corr}) value changed when the concentration of inhibitors was higher than in the uninhibited solution. This study also showed that Comp-1 (87 mV) and Comp-2 (86 mV) had the highest displacement in E_{corr} values, which proved that the inhibitors were mixed-type. The difference between the (E_{corr}) values in the presence and absence of an inhibitor showed that the (E_{corr}) value was less than, which is a crucial point to explain whether the (E_{corr}) value changes (-89 mV). Additionally, this study revealed that the anodic dissolution at the anode and hydrogen evolution at the cathode was crucial, as indicated by the changes in the a and c values in the presence of the inhibitor, compared to when it was absent [24].

On the other hand, Fig. 6 a and b show that the corrosion rate values (CR) went down as the concentrations of all TM inhibitors (Comp-1 and Comp-2) increased compared to when there were no inhibitors. This work also confirmed that the surface coverage (θ) and inhibition efficiency (IE%) values have also been subjected to the corrosion rate [25]. Similarly, the efficiency of the inhibition revealed an increase with increasing inhibitor concentration (Fig. 6 c and d) [26]. Finally, it was noted that at a concentration of 25 ppm, the values of (% IE) and (θ) for the synthesized inhibitors (Comp-1 and Comp-2) were around (70.4 %, 0.7), and (81.7 %, 0.81), respectively.

The inhibition efficiency of the synthesized inhibitors (Comp-1 and Comp-2) was calculated using the following equation [27]:

$$CapIE = \frac{CR^o - CR}{CR^o} \times 100\%, \quad (1)$$

where CR and CR^o are corrosion rate un-inhibited and inhibited complexes, respectively, $IE\%$ is inhibitor efficiency.

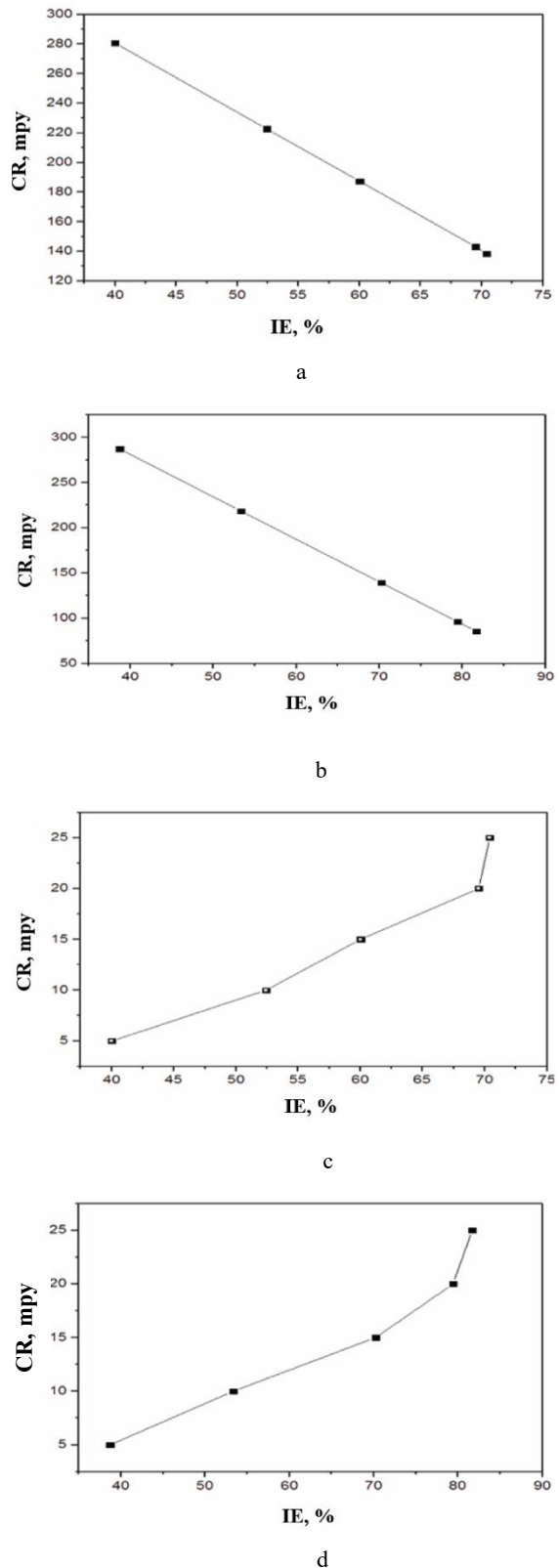


Fig. 6. a, b– the relationship between corrosion rate and efficiency of Comp-1 and Comp-2 at 298 K, respectively; c, d– the relationship between concentration and efficiency of Comp-1 and Comp-2 at 298 K, respectively

4. CONCLUSIONS

During this study, trimethoprim TM and its derivatives were synthesized, proving suitable inhibitors of carbon steel alloys. Further investigations revealed that these inhibitors have enhanced inhibition efficiency with increasing concentration. Additionally, the results verified that at a concentration of 25 ppm, the inhibition efficiency of Comp-2 (81.7 %) surpasses that of Comp-1 (70.4 %). The UV-visible results confirmed that two transitions (n and T2-E) happen in the spectral regions of 200–400 nm and 400–800 nm. These bands were considered potential bands due to ligand field and charge transitions. TGA results confirmed various weight losses due to the loss of water molecules and multiple groups. About 13.98 %, 24.92 %, 93.32 %, 30.25 %, and 51.32 % of the weight was lost, and the findings were closely aligned with the theoretical values. This shows that the synthesized complexes have a lower corrosion rate. Similarly, FTIR and polarization study results have demonstrated significant compatibility among the previous studies made during this research work.

REFERENCES

1. **Miller, R.B., Lawson, K., Sadek, A. Monty, C.N., Senko, J.M.** Uniform and Pitting Corrosion of Carbon Steel By *Shewanella Oneidensis* MR-1 Under Nitrate-Reducing Conditions *Applied and environmental microbiology* 84 (12) 2018: pp. e00790-18. <https://doi.org/10.1128/AEM.00790-18>
2. **Jiang, J.Y., Liu, Y., Chu, H.Y., Wang, D., Ma, H., Sun, W.** Pitting Corrosion Behaviour of New Corrosion-Resistant Reinforcement Bars In Chloride-Containing Concrete Pore Solution *Materials* 10(8) 2017: pp. 903. <https://doi.org/10.3390/ma10080903>
3. **Sarmiento, E., González-Rodríguez, J., Uruchurtu, J., Sarmiento, O., Menchaca, M.,** Fractal Analysis of The Corrosion Inhibition of Carbon Steel In A Bromide Solution By Lithium Chromate *International Journal of Electrochemical Science* 4 (1) 2009: pp. 144–155. [https://doi.org/10.1016/S1452-3981\(23\)15143-1](https://doi.org/10.1016/S1452-3981(23)15143-1)
4. **Anaee, R.A.** Sodium Silicate and Phosphate As Corrosion Inhibitors For Mild Steel In Simulated Cooling Water System *Arabian Journal for Science and Engineering* 39 2014: pp. 153–162. <https://doi.org/10.1007/s13369-013-0865-x>
5. **De Ketelaere, E., Moed, D., Vanoppen, M., Verliefde, A.R.D., Verbeken, K., Depover, T.** Sodium Silicate Corrosion Inhibition Behaviour For Carbon Steel In A Dynamic Salt Water Environment *Corrosion Science* 217 2023: pp. 111119. <https://doi.org/10.1016/j.corsci.2023.111119>
6. **Yang, H.M.** Role Of Organic And Eco-Friendly Inhibitors On The Corrosion Mitigation of Steel in Acidic Environments – A State-of-Art Review *Molecules* 26 (11) 2021: pp. 3473. <http://doi.org/10.3390/molecules26113473>
7. **Boughoues, Y., Benamira, M., Messaadia, L., Bouider, N., Abdelaziz, S.** Experimental and Theoretical Investigations of Four Amine Derivatives as Effective Corrosion Inhibitors for Mild Steel In HCl Medium *RSC Advances* 10 (40) 2020: pp. 24145–24158. <http://doi.org/10.1039/D0RA03560B>
8. **Ouakki, M., Galai, M., Rbaa, M., Abousalem, A.S., Lakhrissi, B., Touhami, M.E., Cherkaoui, M.** Electrochemical, Thermodynamic and Theoretical Studies of Some Imidazole Derivatives Compounds As Acid Corrosion Inhibitors For Mild Steel *Journal of Molecular Liquids* 319 2020: pp. 114063. <http://doi.org/10.1016/j.molliq.2020.114063>
9. **Fajobi, M., Fayomi, O., Akande, I., Odunlami, O.** Inhibitive Performance of Ibuprofen Drug on Mild Steel In 0.5M of H₂SO₄ Acid *Journal of Bio-and Tribo-Corrosion* 5 2019: pp. 1–5. <https://doi.org/10.1007/s40735-019-0271-3>
10. **Duca, D., Dan, M., Vaszilcsin, N.** Expired Domestic Drug-Paracetamol-As Corrosion Inhibitor For Carbon Steel In Acid Media *In IOP Conference Series: Materials Science and Engineering* 416 2018: pp. 012043. <http://dx.doi.org/10.1088/1757-899X/416/1/012043>
11. **Al-Amiery, A.A., Mohamad, A.B., Kadhum, A.A.H., Shaker, L.M., Isahak, W.N.R.W., Takriff, M.S.** Experimental and Theoretical Study on The Corrosion Inhibition of Mild Steel By Nonanedioic Acid Derivative in Hydrochloric Acid Solution *Scientific Reports* 12 (1) 2022: pp. 1–21. <https://doi.org/10.1038/s41598-022-08146-8>
12. **Samide, A.** A Pharmaceutical Product As Corrosion Inhibitor For Carbon Steel In Acidic Environments *Journal of Environmental Science and Health, Part A* 48 (2) 2013: pp. 159–165. <http://doi.org/10.1080/03601234.2012.716744>
13. **Albahadly, H.H., Al-Haidery, N.H., Al-Salami, B.K.** Synthesis, Biological Activity of Trimethoprim Derivative and The Complexes *In Journal of Physics: Conference Series* 2063 2021: pp. 012014. <http://doi.org/10.1088/1742-6596/2063/1/012014>
14. **Smith, G.L., Reutovich, A.A., Srivastava, A.K., Reichard, R.E., Welsh, C.H., Melman, A., Bou-Abdallah, F.** Complexation of Ferrous Ions By Ferrozine, 2, 2'-Bipyridine and 1, 10-Phenanthroline: Implication For The Quantification of Iron In Biological Systems *Journal of Inorganic Biochemistry* 220 2021: p. 111460. <https://doi.org/10.1016/j.jinorgbio.2021.111460>
15. **Mostafa, A., El-Ghossein, N., Cieslinski, G.B., Bazzi, H.S.,** UV-Vis, IR Spectra and Thermal Studies of Charge Transfer Complexes Formed In The Reaction of 4-Benzylpiperidine With σ - and π -Electron Acceptors *Journal of Molecular Structure* 1054 2013: pp. 199–208. <http://doi.org/10.1016/j.molstruc.2013.09.007>
16. **Yakan, H.** Novel Schiff Bases Derived From Isothiocyanates: Synthesis, Characterization, and Antioxidant Activity *Research on Chemical Intermediates* 46 (8) 2020: pp. 3979–3995. <http://doi.org/10.1007/s11164-020-04185-w>
17. **Osowole, A.A., Wakil, S.M., Alao, O.K.** Synthesis, Characterization And Antimicrobial Activity of Some Mixed Trimethoprim-Sulfamethoxazole Metal Drug Complexes *World Applied Sciences Journal* 33 (2) 2015: pp. 336–342. <http://doi.org/10.5829/idosi.wasj.2015.33.02.22206>
18. **Nair, M., Putnam, A., Mishra, S., Mulks, M., Taft, W., Keller, J., Miller, J., Zhu, P.P., Meinhart, J., Lynn, D.** Faeriefungin: a New Board-Spectrum Antibiotic From *Streptomyces Griseus* Var. *Autotrophicus* *Journal of Natural Products* 52 (4) 1989: pp. 797–809. <http://doi.org/10.1021/np50064a022>
19. **ElShaer, A., Hanson, P., Worthington, T., Lambert, P., Mohammed, A.R.** Preparation and Characterization of Amino Acids-Based Trimethoprim Salts *Pharmaceutics* 4 (1) 2012: pp. 179–196.

<http://doi.org/10.3390/pharmaceutics4010179>

20. **Wurrey, C., Krishnamoorthi, R., Nease, A.** Vibrational Spectra and Structure of Cyclopropyl Isothiocyanate *Journal of Raman Spectroscopy* 9 (5) 1980: pp. 334–338. <http://doi.org/10.1002/jrs.1250090511>
21. **Ali, A.N., Alaa, S., Hadi, Z.** Synthesis, Characterization and Evaluation of Some Graphene Oxide Derivatives and Their Application As Corrosion Inhibitors For Carbon Steel Alloy Type C1025 In Hydrochloric Acid *International Journal of Corrosion and Scale Inhibition* 8 (4) 2019: p. 974–997. <http://doi.org/10.17675/2305-6894-2019-8-4-11>
22. **Damej, M., Hsissou, R., Berisha, A., Azgaou, K., Sadiku, M., Benmessaoud, M., Labjar, N.** New Epoxy Resin As A Corrosion Inhibitor For The Protection of Carbon Steel C38 In 1M HCl. Experimental And Theoretical Studies (DFT, MC, and MD) *Journal of Molecular Structure* 2022: pp. 132425. <http://doi.org/10.1016/j.molstruc.2022.132425>
23. **Goe, G.** Phosphorous acid Functionalized Graphene oxide By Microwave and Evaluation as Anti-Corrosion inhibitor for carbon steel alloy Type C1025 in HCl Solution *Journal of Kufa for Chemical Science* 2 (6) 2020: pp. 145–165.
24. **Al-Jubanawi, I.M., Al-Sawaad, H.Z., Alwaaly, A.A.** Synthesis Characterization and Corrosion Inhibition of Thiourea and Phthalic Anhydride Complex with Ni (II) for Carbon Steel Alloy C1010 0.1 M Hydrochloric Acid *Surface Engineering and Applied Electrochemistry* 57 (5) 2021: pp. 595–606. <http://doi.org/10.3103/S1068375521050057>
25. **Saraswat, V., Yadav, M.** Improved Corrosion Resistant Performance of Mild Steel Under Acid Environment By Novel Carbon Dots As Green Corrosion Inhibitor *Colloids and Surfaces A: Physicochemical and Engineering Aspects* 627 2021: pp. 127172. <http://doi.org/10.1016/j.colsurfa.2021.127172>
26. **Benzbiria, N., Echihi, S., Belghiti, M., Thoume, A., Elmakssoudi, A., Zarrouk, A., Zertoubi, M., Azzi, M.** Novel Synthetized Benzodiazepine As Efficient Corrosion Inhibitor For Copper In 3.5% NaCl Solution *Materials Today: Proceedings* 37 2021: pp. 3932–3939. <http://doi.org/10.1016/j.matpr.2020.09.030>
27. **Daoud, D., Douadi, T., Hamani, H., Chafaa, S., Al-Noaimi, M.** Corrosion Inhibition Of Mild Steel By Two New S-Heterocyclic Compounds In 1 M HCl: Experimental and Computational Study *Corrosion Science* 94 2015: pp. 21–37. <https://doi.org/10.1016/j.corsci.2015.01.025>



© Naser et al. 2024 Open Access This article is distributed under the terms of the Creative Commons Attribution 4.0 International License (<http://creativecommons.org/licenses/by/4.0/>), which permits unrestricted use, distribution, and reproduction in any medium, provided you give appropriate credit to the original author(s) and the source, provide a link to the Creative Commons license, and indicate if changes were made.